Investigation of Space Charge Compensated Transport by Use of a Gabor Plasma Lens

J. Pozimski, R. Dölling, P. Gross, H. Klein
Institut für Angewandte Physik, Frankfurt, Germany

Abstract

Low energy beam transport (LEBT) of high perveance ion beams suffers from high space charge forces. Space charge compensation reduces the necessary focusing force of the lenses and the radius of the beam in the lenses and therefrom the emittance growth due to aberrations and self fields. The use of electrostatic lenses is restricted due to decompensation by the electric fields. On the other side magnetic lenses suffer, for high mass ions, from the necessary high magnetic fields and the resulting technical problems. A different approach for LEBT is a lens using a static non neutral plasma confined in a magnetic and electrostatic field configuration allowing strong electrostatic focusing with only small influence on space charge compensation. Modeling of the plasma in respect to low lens aberrations is very difficult and there is no closed theory available. New measurements at low residual gas pressure as well as theoretical work will be discussed.

Introduction

For prediction of the transport capabilities of a low energy transport line using compensated transport it is necessary to know the density distributions of the compensating particles and the beam particles. So far the distribution of the compensating particles can only be calculated in a selfconsistent way, in a drift region [1,2,3]. This is not possible inside magnetic structures now. The theory for determination of the electron density (for positive ions) in compensated transport might benefit from the theory of charge density distribution in a Gabor plasma lens (GPL) where the electron enclosure is performed by magnetic and electrostatic fields. The advantages of a Gabor lens for measurements are higher electron densities and therefore enhanced influence on the beam. Therefore solving the density distribution problem for the GPL might be a step forward for description of compensated transport. An indication therefore give [4,5] where some aberrations in compensated transport are explained by a high electron density on axis. Apart from the forecast of self fields in compensated transport the GPL is still a very promising candidate for a LEBT line.

Theory

The theory of ·electron density in a Gabor lens was originally given by [6]. The maximum density is only determined by the (homogeneous) magnetic field and given by

$$\rho_{e\max} = \frac{e \cdot \varepsilon_0 \cdot B_z^2}{2 \cdot m_e} \qquad (1)$$

Other studies [7,8] assume that the focal strength of a Gabor lens is linear with the applied electric potential of the center electrode. Results of numerical calculations using eq. (1) for the radial

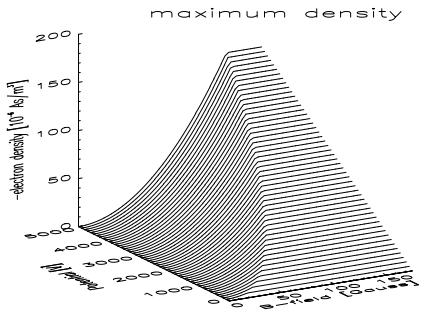

Fig. 1: Theoretical maximum electron density in a Gabor lens as a function of the external fields

electron enclosure density and a Poisson solver for the longitudinal confinement by the electrode potential assuming a homogeneous filled cylinder of 106 mm length and 35 mm diameter (this is the free space inside the Frankfurt Gabor lens) is shown in fig. 1. The maximum electron density is a function of the free external field parameters. This calculated theoretical maximum density might not be reached in an experiment. Furthermore a homogeneous density distribution was assumed which has to be proven experimentally.

Experimental set up

Two experiments have been set up. One for determination of the electron density by examination of the light emitted by the plasma. This radiation is produced by collisions between the residual gas and the captured electrons. A second experiment was set up to measure the focusing capabilities of the GPL using a 10 keV He^+ beam. The results will be compared with numerical simulations.

Density measurements

The set up for the measurement of the radial density distribution is shown in fig. 2. The GPL was mounted on a turbo molecular pump with an adjustable valve for residual gas pressure control. The plasma is produced by a gas discharge below the Paschen limit. The emitted light was measured by a CCD camera installed on top of the lens. Therefore the measured light intensity is integrated along the z axis. The results are used to determine the electron density distribution. The pressure was adjusted to be comparable to the beam experiments. Helium, argon and hydrogen where used as residual gas.

Beam measurements

The set up for the measurement of the focusing capabilities is shown in fig. 3. The ion beam (He^+, 10 keV, 4 mA, DC, p = $7*10^{-5}$ hPa) was extracted from a HIEFS [9] like ion

*Work supported by BMBF (contract O6OF359)

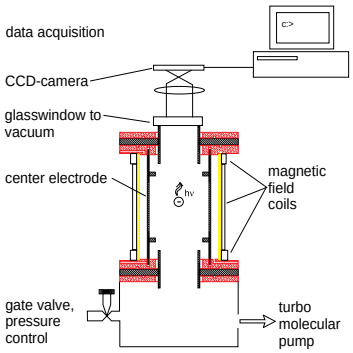

Fig. 2: Experimental set up for the measurement of the light.

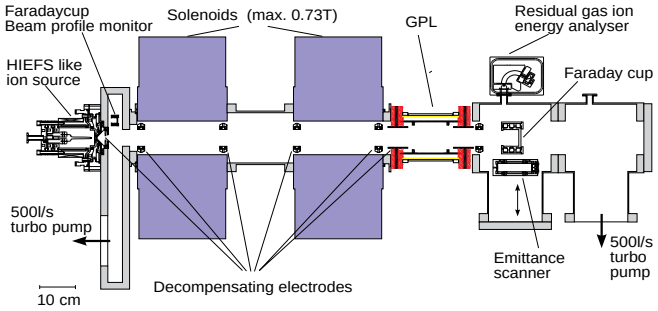

Fig. 3: Experimental set up for beam measurement.

source and a parallel beam of app. 40 mm diameter at the entrance of the Gabor lens was formed by the LEBT consisting of two solenoids. The Gabor lens was followed by a diagnostic tank (profile, beam potential and emittance measurements).

Experimental results

Density measurements

Fig. 4 shows a result of a light intensity measurement. The intensity of the emitted light is strongly peaked on the lens axis and therefrom the electron density is assumed to be distributed in a similar way. In fig. 5 the radial light intensity distribution is shown as a function of the potential on the center electrode, the form of the radial density distribution seems to be constant and the height growths linear in a first approximation except for the lowest fields where the gas discharge is off. In fig. 6 the light intensity is shown as a function of the external field.

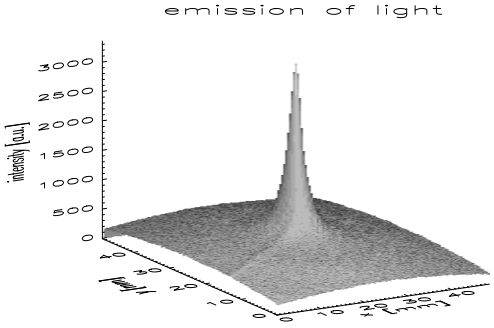

Fig. 4: Intensity of the emitted light as a function of x and y for a CCD exposure time of 5 s and a lens potential of 3 kV and magnetic field strength of 105 G.

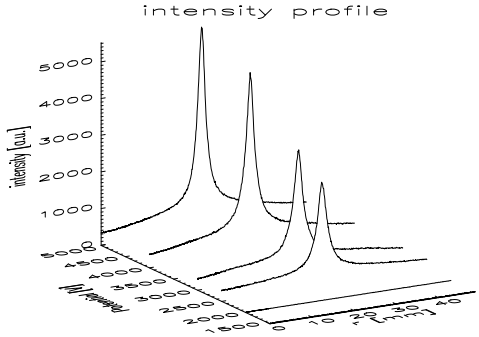

Fig. 5: Radial density distribution of the emitted light as a function of the electrode potential for a fixed magnetic field of 105 G.

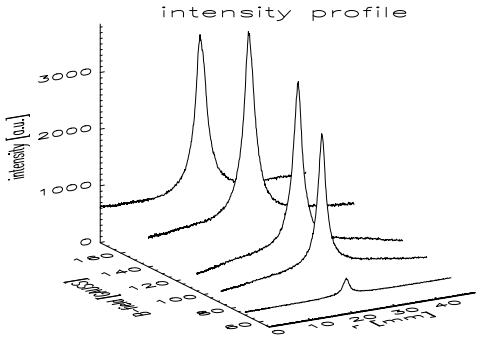

Fig. 6: Radial density distribution of the emitted light as a function of the magnetic field for a fixed lens potential of 3 kV.

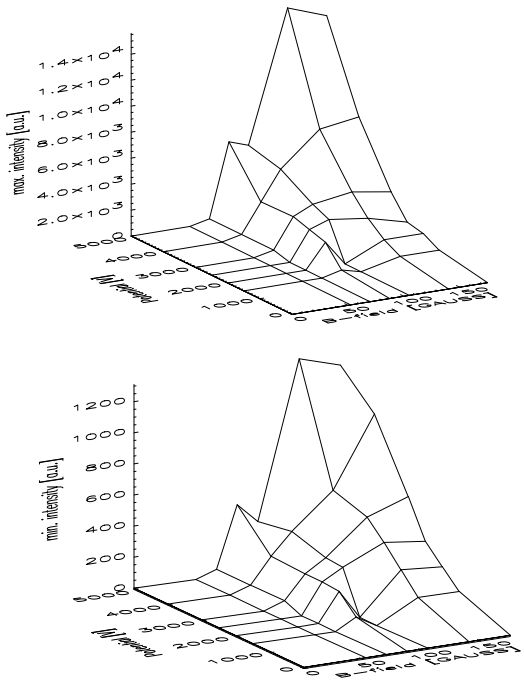

Fig. 7: Maximum and minimum intensity of the emitted light as a function of the electric and magnetic field.

The intensity rises more than linear for low fields and then levels off. In fig. 7 the maximum (upper graph) and the minimum (lower graph) light intensity of the profiles is shown as a function of the external parameters electrode potential and magnetic field

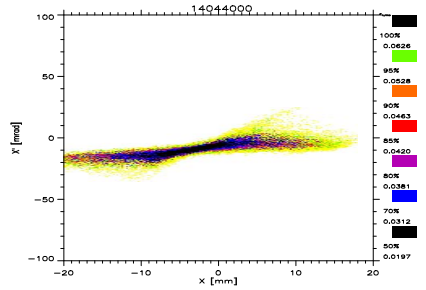

Fig. 8: Emittance behind the not active lens.

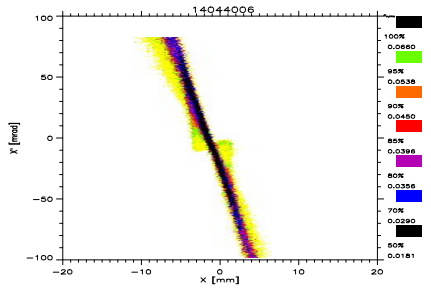

Fig. 9: Emittance behind the lens for 3 kV potential and B=66 Gauss.

strength. The contour of these light intensity plots are similar to the pattern of the theoretical expected maximum electron densities (fig. 1).

Beam measurements

The results of the emittance measurements behind the Gabor lens are shown in fig. 8 and 9. Fig. 8 shows the emittance with the lens off, fig. 9 with the lens in operation. Fig. 10 - 12 show numerical calculations of the transport capabilities of the lens. In fig. 10 the emittance in front of the lens is shown. This was calculated from the measured emittance behind the lens (fig. 8) using 250 beams and neglecting the space charge of the beam (degree of compensation in the measurements was >> 90 %). Fig. 11 shows the result of a transport calculation for operational lens starting with this emittance (fig.10). A homogeneous electron density distribution calculated from the radial limitation criteria for the lens ($\rho_e = 38*10^{-6}$ As/m^3) was assumed. The beam space charge was neglected. Fig. 12 shows the result of a transport calculation using the 'peaked' electron distribution from the CCD measurements scaled to the same density in the maximum ($\rho_{emax} = 38*10^{-6}$ As/m^3).

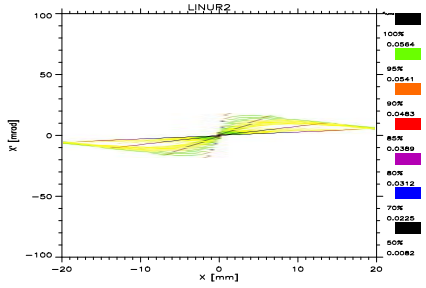

Fig. 10: Reconstructed input emittance (in front of the lens) for numerical simulation of the transport properties of the lens.

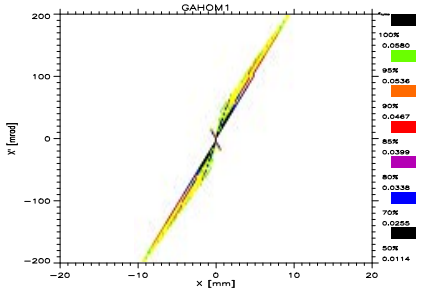

Fig. 11: Numerical simulation of the emittance behind the lens under the assumption of homogeneous distributed electrons.

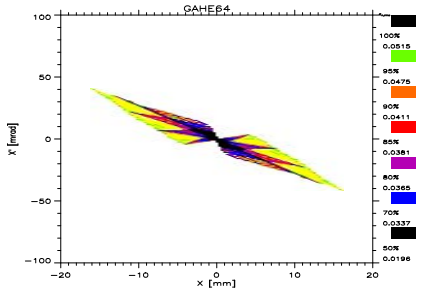

Fig. 12: Like fig. 11 under assumption of peaked electron distribution.

Conclusions

Comparison between the measured emittance and the calculated emittances show in focusing strength and in aberration forecast a better result for the peaked than for the homogeneous distribution. Nevertheless the experiments indicate that the electron density is between these two cases. This could be explained by additional electrons produced by the beam traveling through the lens and the influence of the beam potential on the plasma. The principle for the electron concentration on the axis is unknown. Therefore theoretical work using selfconsistent density distributions for the thermalized electrons will be done.

References

[1] J. Pozimski et. al. GSI-Annual Report 1992, GSI-93-17, p. 38-40

[2] J. Pozimski et. al. Proc. Frascati 1993

[3] R. Dölling, Dissertation, Institut für Angewandte Physik, Univ. Frankfurt (1994)

[4] P. Groß et. al., Proc. LINAC Conf. 1994, Tsukuba

[5] P. Groß, Dissertation in preparation, Institut für Angewandte Physik, Univ. Frankfurt (1996)

[6] D. Gabor, Nature 160 (1947) 89

[7] J. A. Palkovic et. al. Proc. LINAC Conf. 1988, Williamsburg/VA

[8] R. M. Mobley, Brookh. National Lab., BNL-25173 (1973)

[9] K. Volk, Dissertation, Institut für Angewandte Physik, Univ. Frankfurt(1993)

[10] J. Pozimski et. al. GSI-Annual Report 1994, GSI-95-06,p. 32-34

Acknowledgment

We thank L. Wicke and Dr. M. Sarstedt from the IAP for the use of the CCD camera.